Green Chemistry

PAPER

View Article Online
View Journal | View Issue

Cite this: *Green Chem.*, 2025, **27**, 4573

Polyphenol-based fire-resistant coatings: a bio-inspired solution for forest fire prevention†

Mark John Castillo,[a] Jumi Kang,[a] Jinkyu Lim,[b,c] Minok Park *[d,e] and Kyueui Lee *[a,f,g]

Received 6th December 2024,
Accepted 11th March 2025

DOI: 10.1039/d4gc06191h

rsc.li/greenchem

The bark of hardwood trees contains abundant polyphenols, which can rapidly transform into a graphite layer that acts as a thermal barrier, minimizing fire damage. Inspired by this natural fire resistance mechanism, we developed an eco-friendly, cost-effective fire-retardant coating system for forest fire prevention. Comprising only pyrogallol (PG) and polyethyleneimine (PEI), the system forms a polyphenolic layer through oxygen-mediated oxidative crosslinking when exposed to air. This method uses water as the sole solvent and requires no additional catalysts, allowing easy, material-independent application *via* spray-coating. Heat resistance tests showed that the PG–PEI coating improved the wood's inherent fire resistance by approximately threefold, attributed to the rapid coating conversion into a graphite layer at high temperatures, as confirmed by X-ray photoelectron and Raman spectroscopies. Furthermore, a 70-day colorimetric analysis under simulated weathering conditions exposure demonstrated the coating's durability against environmental stresses. The PG–PEI coating also preserved wood's natural functionality, supporting tree health, as evidenced by the high survival rates of the treated trees. These findings suggest the PG–PEI coating is a promising solution for mitigating forest fire damage while maintaining eco-friendliness and practicality.

Green foundation

1. This research advances green chemistry by developing an eco-friendly, cost-effective fire-retardant coating. Mimicking nature's fire-resistance mechanisms, the system eliminates the need for harmful catalysts or solvents and can be easily applied *via* spray coating, supporting sustainable forest fire prevention.
2. The developed coating method enhances the fire resistance of wood by approximately threefold. It forms a protective graphite layer at high temperatures, preserves the functionality of wood, and maintains semi-permanent durability even under environmental stress.
3. Future research could focus on investigating the long-term ecological impact of applying this coating on a large scale in forests.

Introduction

In recent years, unprecedented wildfire seasons have affected nearly every continent, indicating a growing global trend.[1] These fires have resulted in record-breaking pyrogenic carbon emissions and raised serious concerns about the populations of numerous species and ecosystems, highlighting the global impact of forest fires.[2–5] Fire retardants can help decrease the intensity and spread of wildfires, allowing firefighters to establish safe containment lines.[6] For example, cellulose-based hybrid hydrogels exhibit enhanced water-binding, cooling, and sealing properties.[7] Furthermore, ionically crosslinked chitosan-based flame-retardant coatings significantly improve the fire resistance of wood and exhibit self-extinguishing behavior.[8] In addition, polymer composites filled with metal derivatives have gained prominence as flame retardants due to their superior thermal stability and robust fire resistance.[9] The hybridization of metals and polymers imparts favorable

[a]*Department of Chemistry, Kyungpook National University, Daegu 41566, South Korea. E-mail: kyueui@knu.ac.kr*
[b]*Department of Energy and Environmental Engineering, The Catholic University of Korea, Bucheon 14662, South Korea*
[c]*Department of Chemical and Biological Engineering, Hanbat National University, Daejeon 34158, South Korea*
[d]*Energy Technologies Area, Lawrence Berkeley National Laboratory, Berkeley, CA 94720, USA*
[e]*Department of Mechanical and Automotive Engineering, Kongju National University, Cheonan 31080, South Korea. E-mail: minokpark@kongju.ac.kr*
[f]*KNU Institute of Basic Sciences and KNU G-LAMP Project Group, Kyungpook National University, Daegu 41566, South Korea*
[g]*Biomedical Research Institute, Kyungpook National University Hospital, Daegu 41940, South Korea*
† Electronic supplementary information (ESI) available. See DOI: https://doi.org/10.1039/d4gc06191h

characteristics for advanced applications; ongoing research in this domain is driven largely by safety concerns regarding human life and the protection of public property.[9] Other materials employed as fire retardants include composites such as nylon and carbon-based materials,[10,11] UV-curable synthetic polymers,[12,13] and organic–inorganic hybrids.[14,15] However, these materials pose a risk of environmental contamination, potential bioaccumulation, and toxicity.[16–20] Furthermore, they are limited to emergency suppression because they cannot remain on vegetation for extended periods under environmental exposure.[21] Therefore, there is an urgent need for long-lasting, eco-friendly wildfire prevention materials.

Certain tree species possess inherent fire resistance mechanisms because their bark can insulate the cambium; in particular, thick-barked hardwoods provide effective fire protection.[22] Hardwood species such as *Quercus candicans* and *Quercus laurina* have relatively high polyphenol (tannin) concentrations of 8% and 10%, respectively.[23] Species such as the giant sequoia and Canary pines are known for their natural fire retardancy due to their high polyphenol content.[24] The fire-retarding properties of polyphenols stem from their ability to transform into graphitic materials when heated.[24] These graphitic materials serve as protective char barriers, dissipating heat away from ignition and combustion because of their low flammability and high thermal stability.[24,25] However, most tree species lack inherent fire resistance, making the application of fireproofing compounds crucial. Since the tannins in hardwood bark convert into graphitic structures with fire-resistant properties when burning, we hypothesized that applying a polyphenolic coating on the outer layer of non-fire-resistant wood can help prevent wildfires by mimicking these natural defense mechanisms.

A synthetic polyphenol with a structure similar to that of tannins has been recently developed using pyrogallol (PG) and polyethyleneimine (PEI).[26] The amine-functionalized polymer (*i.e.*, PEI) and the phenolic cross-linker (*i.e.*, PG) undergo an ambient oxygen-derived oxidative cross-linking reaction when combined, rapidly forming a polyphenolic layer (PG–PEI).[27,28] This synthetic polyphenol has inherent molecular adhesiveness due to its gallol functionality, which allows for various chemical interactions, including hydrogen bonding, π-related bonding, metal coordination, and charge interactions,[29] enabling it to coat the surface of various substrates. The adhesion between PG–PEI and neighboring substrates is both rapid and strong, particularly with natural products containing proteins[30,31] and nucleic acids.[32] This strength stems from the formation of Schiff bases between the nucleophilic groups (amines and thiols) and gallol functional groups, which creates strong covalent bonds. Consequently, the PG–PEI film can be applied to natural-derived materials, such as wood, and it will remain consistently on the coated surface.

We hypothesize that similar to polyphenol-rich bark, PG–PEI-coated woods will exhibit fire-resistant properties when exposed to high temperatures. Previous studies have demonstrated that PG–PEI films can be thermally annealed to convert them to graphitic materials with properties similar to those of graphene.[33] During carbonization, the oxygenated defects on the sp^2 carbon plane are removed, converting polyphenols to graphitic materials. This phenomenon has also been observed in other synthetic polyphenols, such as polydopamine, where it enhances their physicochemical properties.[34] Thus, applying PG–PEI-based polyphenols on wood surfaces could reduce wildfire spread, protect natural ecosystems, and safeguard human communities in fire-prone areas.

Herein, we present a PG–PEI spray coating that functions as an effective fire retardant for forest fire prevention. When coated on non-fire-resistant woods, the PG–PEI coating transforms into a graphitic material with enhanced thermal resistance when exposed to high temperatures. This transformation enhances the fire defense capabilities of trees, as confirmed by heat resistance tests using thermogravimetric analysis (TGA), simulated fire tests, and cone tests. Additionally, the coating demonstrates high chemical stability, maintaining its integrity and protective properties under different weathering conditions for extended periods (70 days). This eco-friendly solution leverages the inherent advantages of polyphenolic materials, offering substantial potential for effective forest fire prevention and enhanced forest management practices.

Experimental

Materials

PG and PEI solutions (50%) were purchased from Sigma-Aldrich (Steinheim, Germany). Cellulose nanofibers (CNFs) were purchased from CNNT (Suwon, South Korea). Red pine wood boards were obtained from Handsu (Seoul, South Korea). Acacia, birch, cedar, cypress, and ficus wood blocks were obtained from PaintInfo (Daejeon, South Korea). Five-year-old pine tree saplings were sourced from Evergreen Farm (Geoje, South Korea). The fire-retardant coatings used in the fire test were obtained from JeilChem (Busan, South Korea), and HyuChemPlus (Gimpo, South Korea).

PG–PEI-coated wood block sample preparation

To prepare a 0.2 M PG solution, 2.52 g of PG was dissolved in 100 mL of deionized water. a 10% PEI solution was created by diluting the 50% PEI solution, which was prepared by mixing 20 mL of 50% PEI with 80 mL of DI water. The prepared solutions were then transferred to separate containers. Wood blocks were evenly spray-coated with the 1 : 1 PG–PEI and subsequently air-dried for 1 hour.

Water contact angle measurement and hydration test

The wettability of the coated sample surfaces was assessed with a contact angle meter (Phoenix 10, SEO, Suwon, South Korea) using the sessile drop method. The substrates, which included representative polymers, metals, glass, silicon wafers, and the different wood samples (acacia, birch, cedar, cypress, ficus, and red pine), were prepared and placed on the contact angle equipment. A droplet of DI water was applied on the surface of the substrates. Five PG–PEI-coated and uncoated

samples were prepared, and their water contact angles (WCAs) were measured using Surfaceware9 (SEO, Suwon, South Korea). All measurements were conducted at room temperature. The average WCA for each control and experimental sample was determined from the five measurements. For the hydration test, tree bark was collected and cut into 5 cm segments. Five control samples and five PG–PEI-coated bark samples were prepared. The initial weight of each sample was measured and averaged to determine the mean initial weight. Subsequently, the samples were placed near a window for 24 hours to expose them to outdoor environmental conditions. Thereafter, the final weight of each sample was measured and averaged to determine the mean final weight. An unpaired *t*-test was conducted to evaluate the significant differences between the control and PG–PEI-coated populations. This statistical test helped determine whether any observed differences in hydration levels and wettability between the control and coated samples were statistically significant. The results provided insights into the effectiveness of the PG–PEI coating in modifying hydration behavior and surface wettability compared to untreated bark.

X-ray photoelectron spectroscopy analysis

To analyze the elements on the surface of the PG–PEI-coated wood blocks, and the formed graphitic-like layer upon fire exposure of the PG–PEI coating, X-ray photoelectron spectroscopy (XPS) was conducted using a NEXSA XPS system (ThermoFisher, Waltham, MA, United States). A monochromatic X-ray source (Al-Kα) beam was used for data collection. The data were deconvoluted using an Avantage Data System (ThermoFisher, Waltham, MA, USA) to calculate the atomic percentages.

Thermogravimetric analysis and fire test

To analyze the thermal decomposition of the CNFs, PG–PEI, and PG–PEI-CNF, TGA was conducted using an AUTO-Thermogravimetric Analyzer (TA Instruments, New Castle, United States). The analysis was conducted under ambient air conditions with a temperature range of 0–800 °C using a heating rate of 10 °C min^{-1}. This approach allowed for precise measurement of the weight loss of the wood samples as they thermally degraded at increasing temperatures. Additionally, a constant-temperature TGA was performed on CNF and PG–PEI-CNF samples at 300 °C, 400 °C, and 500 °C for a duration of 70 minutes to assess their thermal stability and decomposition behavior at constant temperature. A fire test was conducted using four types of wood samples: bare wood, commercially available fire-retardant-coated wood (Brand X and Brand Y), and PG–PEI-coated wood. A continuous fire source was prepared, and each wood sample was exposed to fire for 1 minute intervals. After each minute of exposure, the sample was weighed to measure its weight loss. This process was repeated for a total of 5 minutes, with the weight loss recorded after each interval. Additionally, a separate fire test was conducted on various types of wood, including acacia, birch, cedar, cypress, and ficus. Both bare and PG–PEI-coated samples were prepared and subjected to continuous firing for 3 minutes, with 1 minute intervals between each phase. Similar to the previous fire test, the samples were weighed before and after exposure to determine the weight loss, which was used as a measure of combustion resistance and the effectiveness of the PG–PEI coating. The test aimed to evaluate and compare the fire resistance capabilities of the different wood coatings under controlled conditions and the effectiveness of PG–PEI coating on different wood types.

Cone calorimeter test

Ficus wood blocks measuring 10 cm × 10 cm × 0.3 cm were prepared for testing. Two bare wood samples and two PG–PEI-coated wood samples were produced, with their weights carefully matched to minimize discrepancies. To ensure consistency, all samples were vacuum-dried in a vacuum oven to remove any residual moisture before undergoing cone calorimeter tests. These tests were performed using a Dual Cone Calorimeter (FTT, West Sussex, United Kingdom) in accordance with ISO 5660-1. A heat flux of 50 kW m^{-2} was applied with the samples oriented horizontally, simulating typical fire conditions under ambient oxygen concentration. This setup allowed for a direct assessment of how the PG–PEI coating enhances the fire resistance of ficus wood compared to the bare samples.

Laser flash analysis

Thermal conductivity and diffusivity of both bare and PG–PEI-coated wood samples were measured using a Thermal Diffusivity and Conductivity Measurement System (Netzsch, Selb, Germany). The samples, which had a density of 0.369 g cm^{-3}, were analyzed *via* Laser Flash Analysis (LFA). In this method, a xenon flash lamp emitted a pulse of energy that rapidly heated the sample surface, while an infrared detector on the opposite side recorded the temperature response. The laser voltage was set to 230 V, and the testing was conducted at 250 °C, just before the bare wood samples began to burn.

Raman spectroscopic analysis

The successful graphitization of the PG–PEI coating upon heating was verified through Raman spectroscopy using a Renishaw Raman spectrometer (inVia Reflex model, Wotton-under-Edge, United Kingdom). Three random spots on each sample were analyzed using a laser wavelength of 785 nm. The spectral data with the highest resolution were selected to compare the D and G peaks of each sample. This analysis aimed to characterize the structural transformation of the coating into a graphitic material by assessing the presence and intensity of key spectral features indicative of graphitization.

Influence of coating thickness and environmental conditions on graphitization rate

Wood blocks were coated with multiple layers of PG–PEI, allowing each layer to fully dry before applying the next. Coating thickness was measured using an inverted microscope (Nikon Eclipse TS2, Nikon Instruments, New York, United

States). After coating, the sample surfaces were burned. Additionally, separate sets of samples with a single coating layer were exposed to and burned under different simulated conditions—ambient air (20.9% O_2), oxygen-deprived (8.9% O_2), and high humidity (85% RH). Following these exposures, the extent of graphitization on the PG–PEI-coated surfaces was evaluated *via* Raman spectroscopy (Renishaw inVia Reflex, Wotton-under-Edge, United Kingdom). Spectra were collected at three random spots on each sample using a 785 nm laser. The I_D/I_G ratios were then compared to assess graphitization, and the highest-resolution spectra were selected for detailed analysis.

Pine tree survival rate

A detailed simulation was conducted to verify the effects of the coating on the survival or physiology of the treated trees. Eleven Korean pine trees (*Pinus koraiensis*) were planted, with five serving as control samples and the remaining six being spray-coated with PG–PEI. The survival rate of the trees was continuously monitored weekly for 70 days. The survival of the trees was assessed based on their physical appearance, including signs of health and vitality, such as leaf color, presence of new growth, and overall vigor. Detailed photographs documenting the condition of each tree were captured at each observation point.

Coating color intensity analysis

To determine whether the coating degrades over time, a color intensity test was conducted using a Color Picker application to obtain the RGB values of the coating on the trees. The color intensity was measured every 2 weeks for 70 days. It was calculated using the formula $(IB_{Blank} - IB)/255$, where IB_{Blank} is the blue intensity of the uncoated surface (control), and IB is the blue intensity of the coated surface. The blue value was used because it is the opposite of brown (the coating color). The measured color intensity values of the six PG–PEI-coated samples were averaged, and the standard deviation was computed. A one-way ANOVA with multiple comparisons was conducted to verify if there was a significant difference in color intensity between the coatings on day 1 and other days (*e.g.*, day 14 and day 28). The day 1 data served as the baseline for comparison to assess whether the color intensity of the coating decreased with time.

Weathering resistance test

To assess the durability of PG–PEI and commercially available fire-retardant coatings, various weathering conditions were simulated. Wood blocks (1 cm × 1 cm × 0.2 cm) were coated and subjected to freeze-thaw cycles—three cycles of 10 minutes each, separated by 10 minute intervals, for a total duration of 60 minutes. UV exposure was performed using a VL-4.LC UV lamp (Vilber Lourmat, France), emitting 365 nm and 254 nm wavelengths to replicate sunlight exposure. Additionally, a water submersion test was conducted by immersing the coated samples in deionized water at 25 °C for 24 hours, maintaining a sample-to-water ratio of 1 g : 1 L. After exposure to these conditions, surface morphology changes were analyzed *via* a Field Emission Scanning Electron Microscope (FE-SEM) (Hitachi, Tokyo, Japan) to evaluate the coatings' structural integrity and degradation.

VOC emission analysis by gas chromatography

A volatile organic compound (VOC) emission analysis was performed using a Gas Chromatography-Mass Spectrometry (GC-MS) system (Agilent, Santa Clara, CA, USA) to compare emissions from burned bare wood and PG–PEI-coated wood. Both samples were combusted under identical conditions, followed by a 30 minute sample extraction. The analysis was conducted at a maximum temperature of 240 °C with a split ratio of 20 : 1, employing a DB-WAX column (Agilent 122–7062; 60 m × 250 μm × 0.25 μm) for separation. The total run time was 103 minutes.

Elemental analysis by ICP-OES

Coated samples were submerged in deionized water at 25 °C for 24 hours, maintaining a constant sample-to-water ratio of 1 g : 1 L to facilitate the extraction of soluble components. The resulting extracts were then analyzed using inductively coupled plasma optical emission spectroscopy (ICP-OES) (PerkinElmer, Springfield, United States) to determine the presence and concentration of elements commonly associated with fire-retardant coatings. The analysis targeted Al, As, Cd, Co, Cu, Fe, Mn, Mo, Ni, P, Ti, V, and Zr. Elemental concentrations below 0.005 ppm were considered nondetectable, ensuring precise evaluation of the metallic and non-metallic components in the coating.

Cytotoxicity analysis

A cytotoxicity test was performed using MC3T3-E1 cells to confirm the biocompatibility of just PG–PEI coating film and ashes from bare wood, PG–PEI-coated wood, and PG–PEI film. PG–PEI film sample was prepared by combining PG–PEI and cellulose to mimic the tree structure. The resulting PG–PEI-CNF film was washed with Dulbecco's PBS for 24 h. Subsequently, the film was placed in a conical tube with an alpha MEM and incubated for 24 h. The ashes were prepared by burning bare wood, PG–PEI-coated wood, and PG–PEI film, then were extracted in an alpha MEM and incubated for 24 hours as well. The MC3T3-E1 cells were maintained in standard media at 37 °C in a humidified 5% CO2 incubator. After 88 h, the cells were harvested and added to the incubated αMEM at various concentrations (0.313 mg mL^{-1}, 0.625 mg mL^{-1}, and 1.25 mg mL^{-1}). These cell suspensions were then seeded into a 96-well plate at a volume of 100 μL per well, with six wells per concentration. After 24 hours, the original media were replaced with Alpha MEM extracts obtained from the samples. The treated cells were incubated in a humidified 5% CO2 incubator at 37 °C for 48 hours. Cytotoxicity was assessed using a CCK-8 assay kit, and the absorbance was measured at 450 nm using a Microplate Reader (Infinite 200 Pro, Tecan, Männedorf, Switzerland).

Cost analysis

A comparative cost analysis was conducted between the PG–PEI coating and two commercially available fire retardants (Brand X and Brand Y). Four wood samples (1 cm × 1 cm × 0.2 cm each) were coated with their respective formulations, following the manufacturer's instructions for the commercial products and our method for PG–PEI. The volume of coating applied (in milliliters) was recorded for each sample. The following formula was subsequently used to calculate the coating cost per square meter (USD per m^2).

$$\text{Cost (USD per m}^2) = \frac{\text{coating used } (mL) \times \dfrac{\text{total price (USD)}}{\text{total coating volume (mL)}}}{\text{area coated } (m^2)}$$

Results and discussion

As shown in Fig. 1a, we developed a fire-retardant spray coating inspired by the natural defense mechanisms of hardwood trees, which use polyphenols to resist fire. Specifically, we employed a synthetic polyphenol, PG–PEI, which rapidly forms on substrates through oxidative cross-linking between PG and PEI. The coating process involves spray coating the bark with a 0.2 M solution of PG and 10% PEI combined in a 1 : 1 ratio. Upon exposure to an oxygen-rich environment, cross-linking occurs, resulting in the formation of a strong, adhesive film.[29–32] The PG–PEI coating can be applied to a wide variety of substrates because of its robust adhesion properties.

To demonstrate the material-independent coating ability of PG–PEI, we performed contact angle measurements before and after applying the PG–PEI coating on various substrates, including metals (*i.e.*, Au, Al, and Cu), polymers (*i.e.*, poly-L-lactic acid [PLLA] and polydimethylsiloxane [PDMS]), glass, and silicon wafers (Fig. S1†). After applying the PG–PEI coating, the contact angles on all the substrates decreased significantly. Specifically, the contact angles for Al, Au, and Cu decreased from 94°, 67°, and 70° to 52°, 39°, and 30°, respectively. The contact angles for PDMS and PLLA also decreased from 82° and 81° to 26° and 38°, respectively. Similarly, the contact angles for the glass and Si wafers decreased from 52° and 69° to 43° and 39°, respectively. These results confirm that the PG–PEI coating successfully altered the surface wettability of the substrates, demonstrating its effective application across various materials.

Considering that the PG–PEI coating modifies inherent surface properties and can be applied on various substrates, we hypothesized that it might also be effective for coating trees

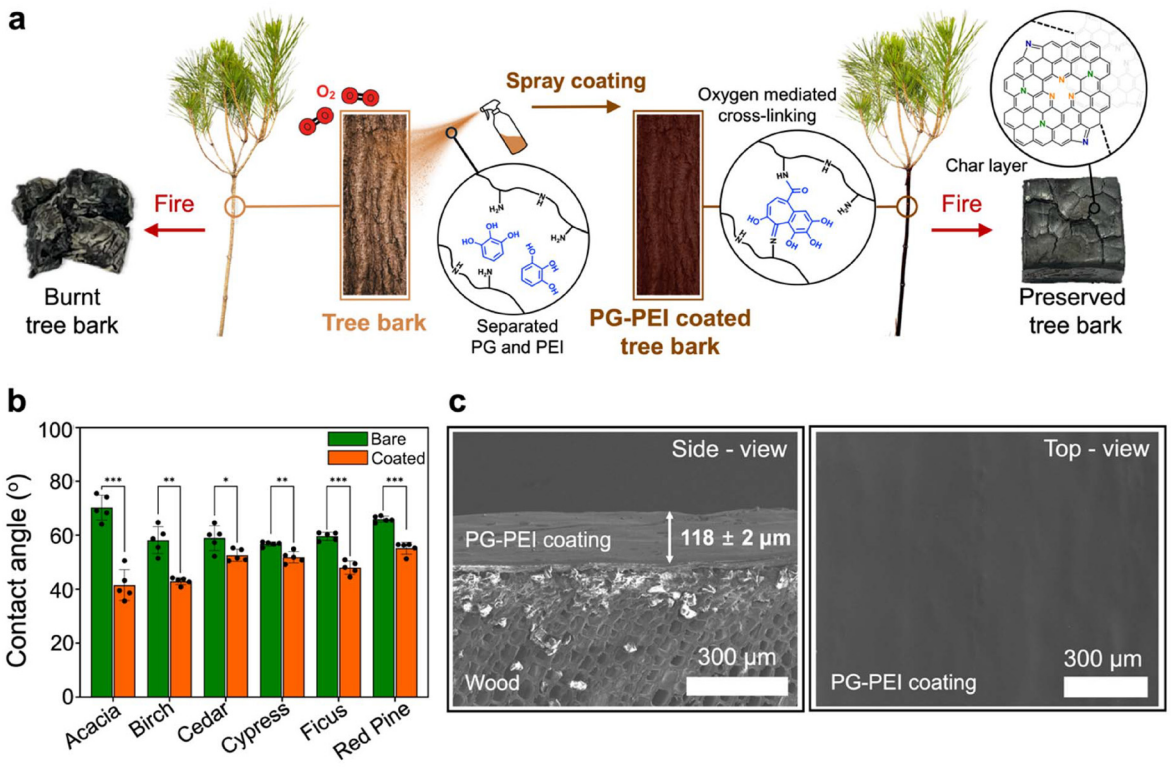

Fig. 1 (a) Schematic illustrating the utilization of a PG–PEI fire-retardant layer for forest fire prevention. The PG–PEI layer can be spray-coated directly onto tree bark through an ambient oxygen-mediated cross-linking mechanism. When burned, the coated layer carbonizes, resulting in a graphitic material with high thermoresistant properties. (b) Contact angle measurements of various wood blocks—acacia, birch, cedar, cypress, ficus, and red pine—before and after coating them with PG–PEI (*: $p < 0.05$, **: $p < 0.01$, ***: $p < 0.001$; $n = 5$). (c) SEM images of the coated wood displaying both the cross-sectional view and the surface morphology of the PG–PEI coating. The white scale bar is 300 μm.

to impart fire resistance. This hypothesis is based on the coating's ability to form a protective char layer when exposed to heat. This char layer acts as a thermal barrier and mitigates the degradation of tree bark during fire events.

To further demonstrate the wood-independent coating ability of PG–PEI, we measured contact angles on various wood species before and after applying the PG–PEI coating (Fig. 1b). The substrates included acacia, birch, cedar, cypress, ficus, and red pine. Following coating application, all substrates exhibited significant reductions in contact angles, indicating a marked change in surface wettability. Specifically, the contact angles for acacia, ficus, and red pine decreased from 70°, 58°, and 63° to 41°, 44°, and 56°, respectively ($p < 0.001$). Birch and cypress samples showed decreases from 58° and 57° to 42° and 52°, respectively ($p < 0.01$). Finally, the cedar wood block demonstrated a decrease from 58° to 55° ($p < 0.05$). These results confirm that the PG–PEI coating effectively alters surface wettability across diverse tree species, highlighting its successful and consistent application.

In addition, scanning electron microscopy (SEM) analysis validated the successful application of the PG–PEI coating on the wood substrates, revealing a coating thickness of 118 ± 2 μm in the cross-sectional images (Fig. 1c, left). This thickness aligns with the effective range for fire-retardant coatings on wood, which typically spans from several micrometers to approximately two millimeters.[35] Coating thickness at different layer applications was also evaluated (Fig. S2†). Two layers of the PG–PEI coating measured 164 μm, while three

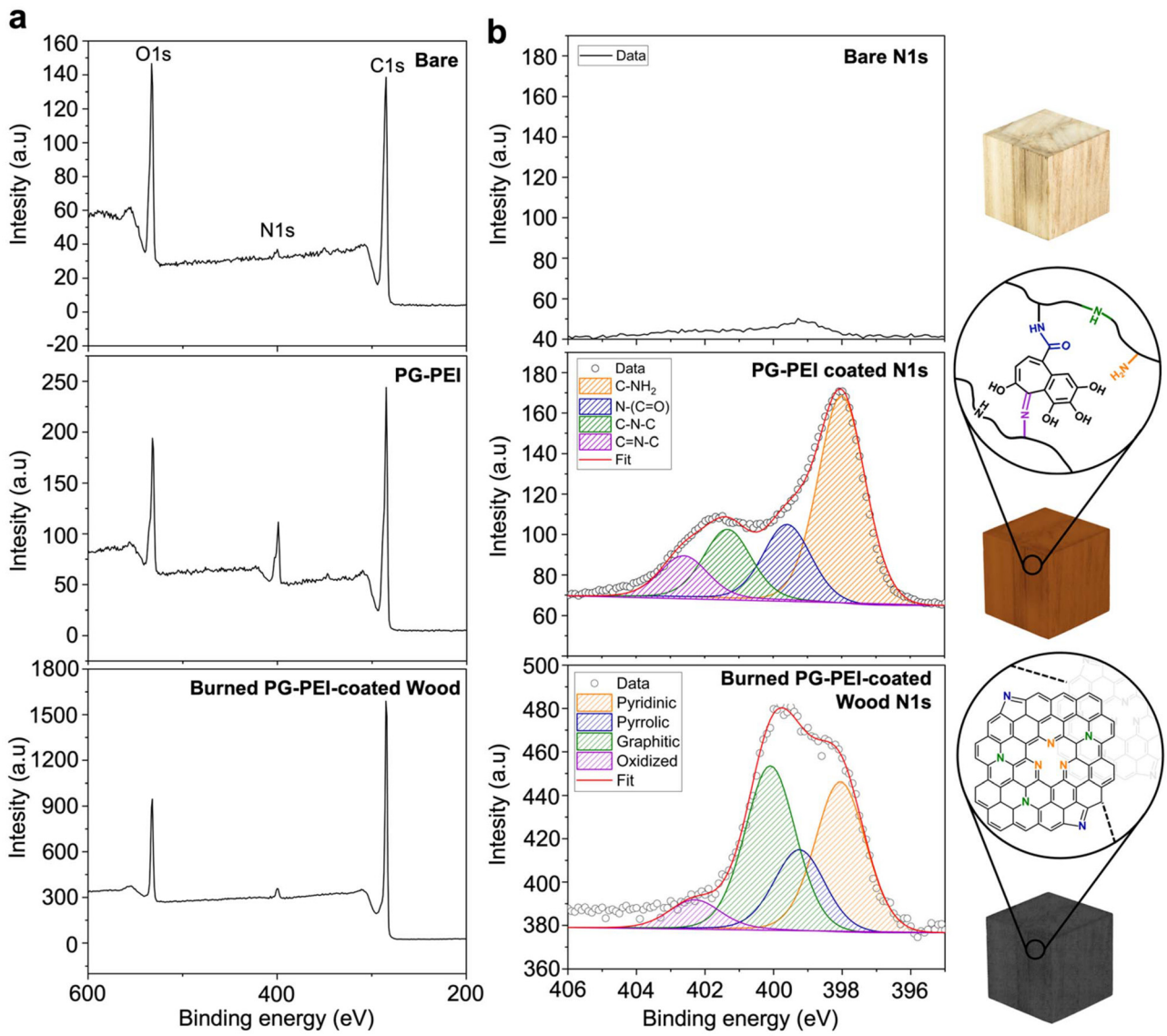

Fig. 2 (a) XPS survey peaks of the bare, PG–PEI-coated, and burned PG–PEI-coated wood blocks, confirming both the successful application of the PG–PEI coating to the substrate and the formation of a graphite-like material upon exposure of the coating to high temperatures. (b) High-resolution N 1s peaks of the bare, PG–PEI-coated, and burned PG–PEI-coated wood blocks, confirming the successful oxidative cross-linking of PG and PEI in the substrate and the formation of graphite material upon fire exposure, respectively.

layers reached 196 μm. These findings confirm that the coating effectively builds up with additional layers. Additionally, the SEM image of the coated wood surface revealed a uniform distribution of the PG–PEI coating across the entire surface (Fig. 1c, right), signifying that the coating provides consistent and comprehensive protection across wood surfaces.

The successful deposition of PG–PEI onto the wood substrate *via* a simple spray application was further confirmed through XPS analysis (Fig. 2a). A comparison of the XPS survey peaks before and after the application of PG–PEI coating revealed that the N 1s peak in the PG–PEI-coated wood block had a much higher intensity than that in the uncoated sample. Specifically, the atomic ratio of C : N : O in the uncoated sample was 73.6 : 1.6 : 24.8, whereas that in the PG–PEI-coated sample shifted to 70.3 : 12.5 : 17.2. This shift is primarily attributed to the introduction of the amine-rich PG–PEI coating. In contrast, the uncoated wood block, which primarily comprised by polysaccharides, exhibited only a minimal N 1s peak because of its ambient organic content. The prominent N 1s signal in the PG–PEI-coated block thereby confirms the successful deposition of the amine-rich PG–PEI coating.

High-resolution analysis of the N 1s peak for the PG–PEI coating confirmed that PG–PEI was chemically cross-linked rather than physically stacked because of the oxidative cross-linking reactions between PG and PEI at the interface (Fig. 2b). Consistent with the survey peak analysis results, the uncoated wood displayed negligible N 1s peaks, whereas the PG–PEI-coated sample exhibited distinct peaks corresponding to nitrogenated functional groups. These peaks included primary and secondary amine groups derived from PEI (green and orange lines in Fig. 2b) and carbon–nitrogen (CN) bonds (blue and purple marks) that may have formed during the cross-linking of the PEI and PG derivatives. Specifically, amine groups corresponding to C–NH_2,[36] N–(C═O) (amide group),[37] C–N–C,[36] and C═N–C (imine)[37] were detected at 398 eV, 399 eV, 401 eV, and 402 eV, respectively. These findings align with previously observed chemical bonds in oxidatively cross-linked PG–PEI,[27] demonstrating that the oxidative cross-linking of PG and PEI occurs rapidly and successfully, even during the short spray application process.

In addition, an XPS survey of the burned PG–PEI-coated wood samples revealed a notable increase in the C 1s peak intensity (Fig. 2a, bottom), with the atomic ratio of C : N : O shifting to 85.1 : 1.8 : 13.2. This shift indicates a substantial rise in carbon content compared with unburned PG–PEI-coated wood, which exhibited a ratio of 70.3 : 12.5 : 17.2. The corresponding decrease in the oxygen and nitrogen peaks suggests that oxygenated and nitrogen-containing defects within the PG–PEI are largely eliminated during thermal treatment, resulting in a carbon-rich layer dominated by graphitic structures.[33] After burning the PG–PEI-coated wood blocks, the chemical composition of the newly formed graphite-like protective layer was analyzed using high-resolution N 1s spectra (Fig. 2b, bottom). Compared to the N 1s spectrum of the unburned PG–PEI-coated wood blocks, the peak positions and relative intensities showed significant differences, indicating that atomic rearrangements occurred during combustion. Specifically, after burning, peaks corresponding to pyridinic (398.0 eV), pyrrolic (399.5 eV), graphitic (401.5 eV), and oxidized (402.5 eV) nitrogen species were observed.[38,39] The presence of these nitrogen functionalities suggests that nitrogen was successfully doped into the graphitic matrix during

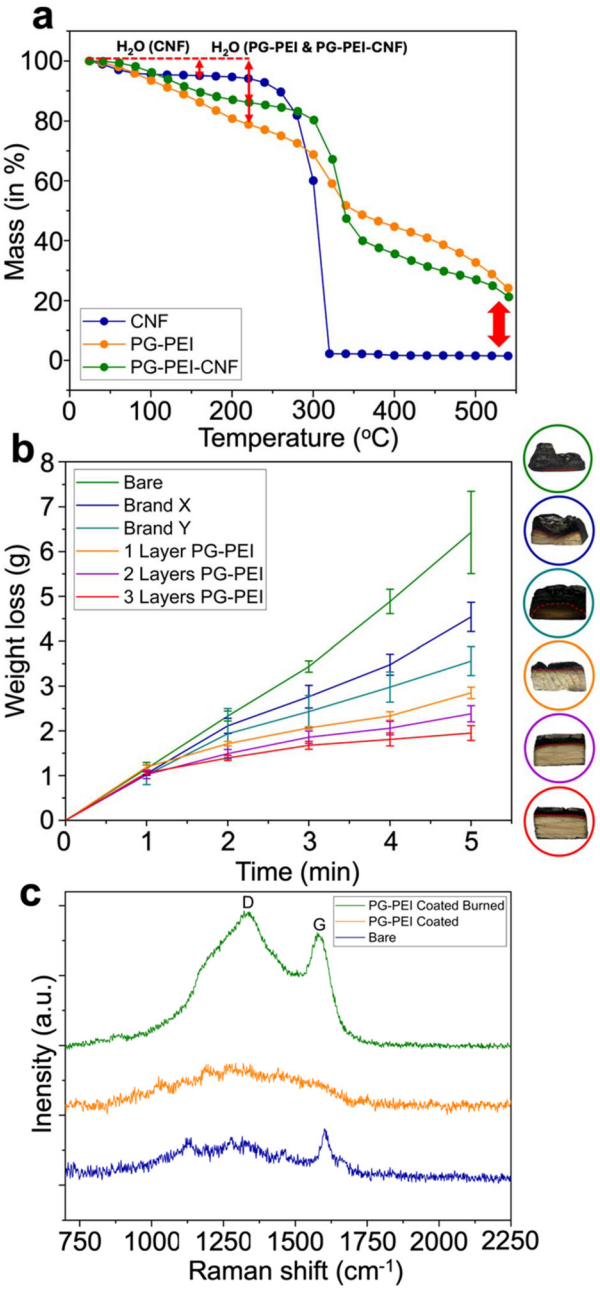

Fig. 3 (a) TGA results of the CNFs, PG–PEI, and PG–PEI–CNF. (b) Fire test results comparing bare wood, commercially available fire-retardant-coated wood blocks (Brand X and Brand Y), and PG–PEI-coated wood blocks with varying coating layers (1, 2, and 3). (c) Raman spectra of the bare, PG–PEI-coated, and burned PG–PEI-coated samples.

thermal conversion, potentially contributing to the improved structural stability and fire resistance of the protective layer.[40]

To assess the effectiveness of PG–PEI as a thermoresistant coating material, TGA was performed to evaluate its thermal stability and degradation behavior at elevated temperatures (Fig. 3a). Specifically, PG–PEI, the CNFs, which represent the natural components of a tree, and PG–PEI-CNF were tested. The PG–PEI and PG–PEI-CNF samples exhibited higher thermal stability than the CNF sample; the former retained their water content up to 220 °C, whereas the latter lost water at 150 °C. Beyond 150 °C, the CNF sample began to degrade, exhibiting a significant weight loss between 290 °C and 313 °C, which is the typical degradation temperature range for cellulose polymeric structures.[41] Conversely, the PG–PEI and PG–PEI-CNF samples exhibited a gradual loss of components within the temperature range of 220–400 °C. Notably, even at temperatures exceeding 550 °C, PG–PEI and PG–PEI-CNF retained 24 wt% and 22 wt% of their components, respectively, whereas the CNFs were completely degraded (Fig. 3a). Additionally, a constant-temperature TGA was performed for 70 minutes at each of the following temperatures—300 °C, 400 °C, and 500 °C (Fig. S3†). At all tested temperatures, PG–PEI-CNF demonstrated significantly enhanced thermal stability compared with CNF. Whereas CNF underwent rapid and complete degradation before reaching the target temperatures, PG–PEI-CNF exhibited a more gradual weight loss, retaining higher thermal resistance. These TGA results demonstrate the effectiveness of PG–PEI as a thermoresistant coating, confirming its potential to enhance the thermal stability and flame retardancy of cellulose-based organisms, such as trees.

Subsequently, we conducted fire tests on bare wood blocks, PG–PEI-coated wood blocks with one, two, or three coating layers, and commercially available fire-retardant-coated wood blocks (Brand X and Brand Y) to evaluate their fire resistance (Fig. 3B). All six samples initially showed similar weight loss during the first minute of continuous fire exposure; this observation can be attributed to the induction time required for graphitization (*i.e.*, char formation) of the PG–PEI coating to develop fully. Once the char layer began to form, the PG–PEI-coated wood blocks exhibited noticeably superior fire resistance compared to the other samples. As shown in Fig. 3B, a distinct difference in weight loss emerged by the two-minute mark and persisted through five minutes. Among the samples tested, the bare wood blocks showed the greatest weight loss overall. Although the commercial products performed better than bare wood, they still did not match the PG–PEI-coated blocks, which demonstrated the highest fire resistance. Moreover, we observed that increasing the number of PG–PEI coating layers led to enhanced fire resistance, underscoring the role of both char layer formation and coating thickness in mitigating combustion. These findings indicate that the fire-retardant effect of the PG–PEI coating is not solely dependent on forming a graphitized char layer on the wood surface; it is also enhanced by the increased char volume contributed by the coating itself, thereby providing more robust protection for the underlying substrate. Additionally, Fig. S4† illustrates the fire performance of PG–PEI-coated and bare wood samples from multiple species (acacia, birch, cedar, cypress, and ficus). Under consistent fire conditions, PG–PEI-coated samples exhibited substantially less weight loss than their bare counterparts, highlighting the coating's effective fire resistance across diverse wood types. These results highlight the exceptional effectiveness of the PG–PEI coating as a fire retardant, which significantly surpasses the performance of both bare wood and commercially available fire-retardant-coated wood. Furthermore, a cost analysis revealed that PG–PEI falls within the price range of commercially available fire retardants, underscoring its affordability (Fig. S5†). Specifically, PG–PEI (32 USD per m^2) is more economical than brand X (40 USD per m^2) and exhibits a statistically comparable cost to brand Y (28 USD per m^2). Consequently, PG–PEI is expected to emerge as a cost-effective, high-performing fire-retardant alternative to existing commercial coatings.

The enhanced fire resistance of the PG–PEI coating is attributable to its transformation into a graphitized char layer

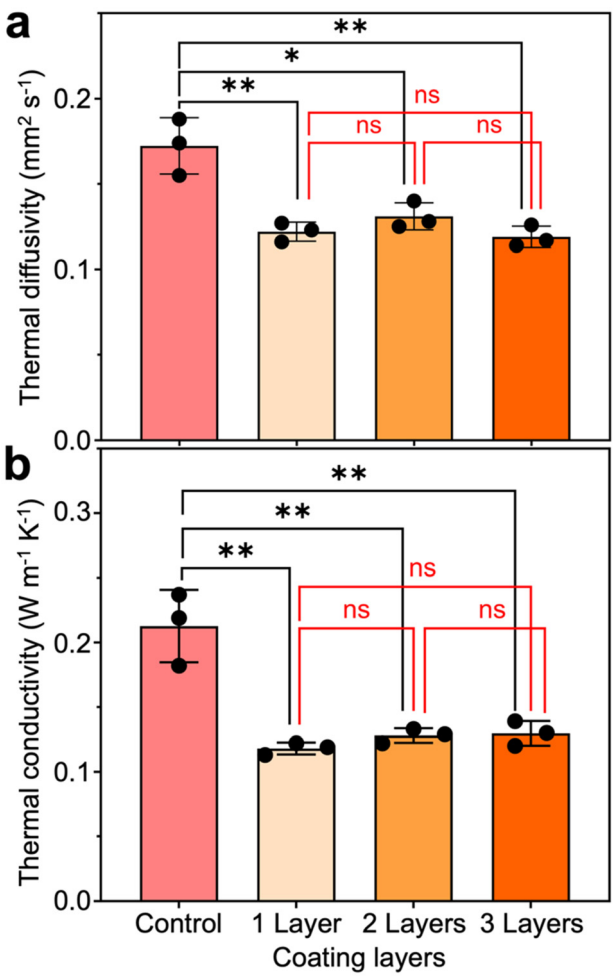

Fig. 4 (a) Thermal diffusivity and (b) thermal conductivity of bare wood and PG–PEI-coated wood samples with 1, 2, or 3 coating layers (n = 3). Statistical significance is indicated as follows: ns = $p > 0.05$, * = $p < 0.05$, and ** = $p < 0.01$.

when exposed to fire. The formation of this graphitized char layer not only prevents further degradation of the underlying wood but also contributes to efficient heat dissipation from the surface.[24,33] This is also evidenced by the Raman spectra (Fig. 3c), where the burned PG–PEI coated samples exhibited distinct D and G peaks, indicative of graphitic structures.[33,42] In contrast, the spectra for the bare wood and the unburned PG–PEI coated samples did not show these peaks, confirming that the graphite-like structures form upon fire exposure. Interestingly, Raman analysis showed no significant change in the I_D/I_G ratio across different coating thicknesses (Fig. S6a†), suggesting that increased thickness does not necessarily enhance the degree of graphitization. Similarly, PG–PEI burned under varying environmental conditions (Fig. S6b†)—ambient air (20.9% O_2), an oxygen-deprived atmosphere (8.9% O_2), and a humid environment (85% RH)—also displayed clear D and G peaks, confirming the formation of a graphite-like protective layer. These findings suggest that, regardless of coating thickness or environmental conditions, PG–PEI consistently forms a protective graphitic layer upon burning.

To understand the thermal barrier mechanisms, we investigated the thermal barrier performance of PG–PEI coatings by comparing a PG–PEI-coated sample with bare wood (control) using laser flash analysis (Fig. 4). As a result, the PG–PEI-coated sample exhibited a thermal diffusivity of 0.1220 mm^2 s^{-1} and a thermal conductivity of 0.118 W m^{-1} K^{-1}, whereas the control showed higher values (0.1723 mm^2 s^{-1} and 0.213 W m^{-1} K^{-1}, respectively). These results demonstrate that the PG–PEI coating substantially reduces heat transfer compared to the control, effectively forming a thermal barrier.

Interestingly, increasing the coating thickness to two or three layers did not significantly alter these thermal properties; both thermal diffusivity and conductivity remained nearly constant. This consistency indicates that the PG–PEI coating provides a reliable thermal barrier effect regardless of thickness, suggesting that even a single-layer PG–PEI coating approximately 100 μm thick (Fig. 1c) is sufficient to achieve effective thermal insulation.

To mimic practical fire scenarios, we prepared 10 × 10 cm^2 wood samples with and without a PG–PEI coating and performed cone calorimeter measurements to evaluate their combustion behavior. Fig. 5 and Table 1 summarize the results, demonstrating significant improvements in fire resistance for the coated sample. Fig. 5a presents the heat release rate (HRR) curves for both samples. The initial HRR peaks occur at 25 seconds, with the bare sample reaching approximately 200 kW

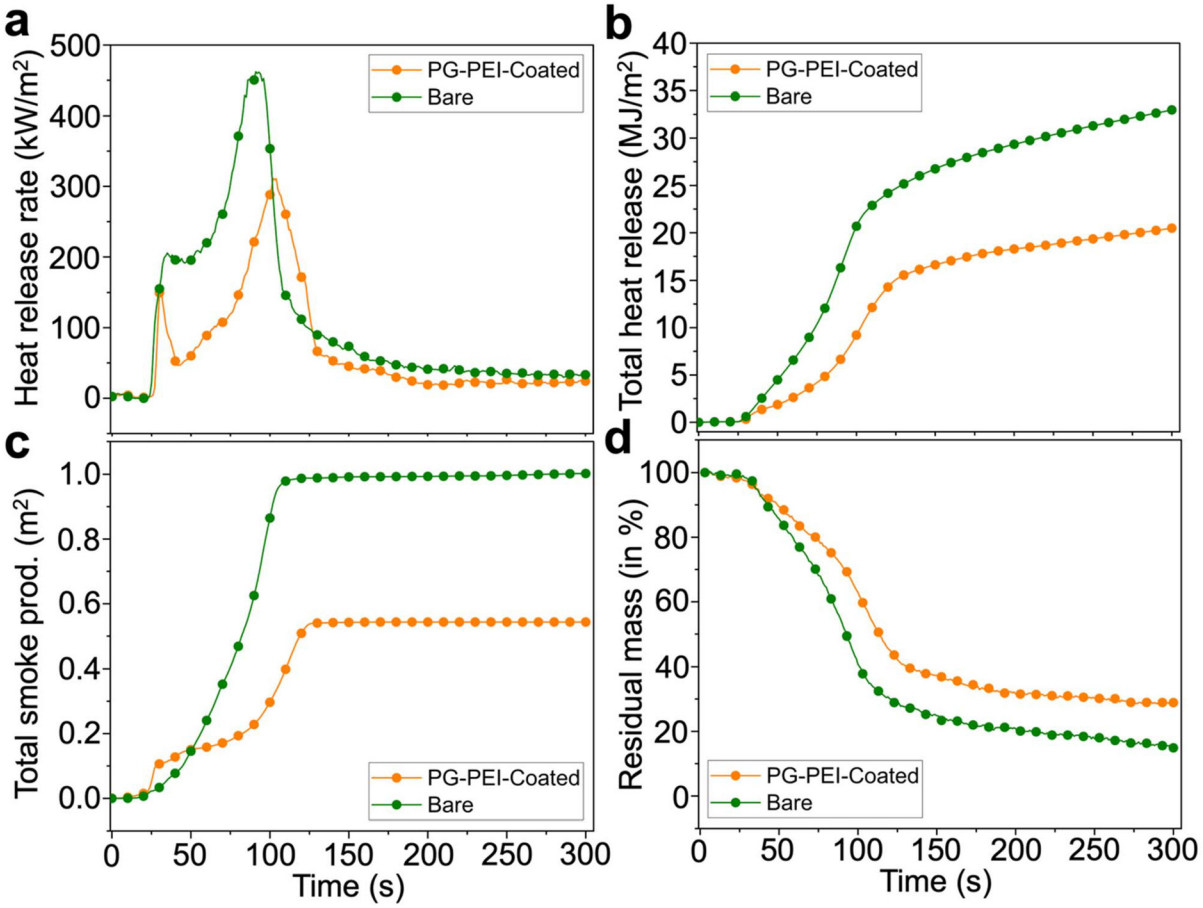

Fig. 5 Cone calorimeter test results comparing bare and PG–PEI-coated wood blocks: (a) heat release rate (HRR, kW m^{-2}), (b) total heat release (THR, MJ m^{-2}), (c) total smoke production (TSP, m^2), and (d) residual mass (%) measured throughout the test.

Table 1 Summary of cone calorimeter data for bare and PG–PEI-coated wood blocks

Sample	Bare	PG–PEI
TTI (s)	23 ± 0.00	25 ± 1.41
Peak HRR (KW m^{-2})	406.14 ± 39.67	325.66 ± 9.93
Mean HRR (KW m^{-2})	69.64 ± 2.66	55.45 ± 5.20
THR (MJ m^{-2})	40.15 ± 1.59	31.90 ± 3.04
TSP (m^2)	1.35 ± 0.25	0.8 ± 0.21
CO_2 production (kg kg^{-1})	1.51 ± 0.01	1.27 ± 0.02

m^{-2} and the coated sample peaking at approximately 150 kW m^{-2}. This approximately 25% reduction in the initial peak HRR indicates that the PG–PEI coating effectively mitigates heat release during the early stages of combustion.[43] The second HRR peak for bare wood occurs at 85 seconds, reaching approximately 450 kW m^{-2}, whereas the coated wood exhibits a delayed second peak at 100 seconds, with a value of approximately 310 kW m^{-2}. This shift in timing and reduction in peak HRR suggest that the coating provides a protective barrier, thereby delaying combustion of the underlying wood substrate.[44] This conclusion is further supported by the total heat release (THR), shown in Fig. 5b. The PG–PEI-coated sample exhibited a THR of 31.90 MJ m^{-2}, compared to 40.15 MJ m^{-2} for the bare sample, representing a 20.5% reduction in overall heat release. This lower THR indicates improved fire resistance and reduced potential for fire spread in the coated wood. In addition, the PG–PEI-coated sample exhibited a shorter time to ignition (TTI) than the bare sample, further demonstrating the coating's effectiveness (Table 1).

Fig. 5c further illustrates the impact of the PG–PEI fire-retardant coating on smoke generation. Overall smoke production for the coated sample decreased, with a total smoke production of 0.80 m^2—a 40.7% reduction compared to the bare sample's 1.35 m^2 (Table 1). Notably, minimal differences in smoke release were observed between the two samples for approximately the first 50 seconds after ignition, but a marked divergence emerged beyond 100 seconds (Fig. 5c). This result can be attributed to the fact that smoke generation remains similar until graphitization begins; once a protective graphitic layer has formed, smoke production is effectively suppressed. In particular, when PG–PEI coating was applied, CO_2 emissions decreased to 1.27 kg kg^{-1}—a 15.9% reduction compared to the uncoated sample (1.51 kg kg^{-1}, Table 1). This finding indicates that PG–PEI coating can also help reduce carbon emissions.

Fig. 5d illustrates the mass loss behavior of both samples, revealing that the coated sample retained more residual mass throughout the experiment. This higher mass retention indicates that the PG–PEI coating fosters the formation of a thermally stable char layer, which minimizes substrate degradation under high temperatures. As a result, the coated wood experiences less overall mass loss, underscoring its enhanced fire resistance and improved structural integrity during combustion. In summary, the PG–PEI coating significantly enhances the fire resistance of wood by promoting char formation and reducing heat release, thereby delaying ignition, suppressing smoke production, and lowering CO_2 emissions.

The ability of a tree to absorb moisture is essential for its survival, and any applied coating should not hinder this ability. To evaluate this, a hydration test was performed on tree bark samples coated with PG–PEI. The samples were coated, allowed to dry, and then exposed to an open environment to absorb moisture for 24 hours. Fig. 6a presents the evaluated hydration capabilities of both the bare and PG–PEI-coated wood bark samples. Although the bare wood absorbed slightly more moisture than the PG–PEI-coated wood, the unpaired *t*-test revealed no statistically significant difference ($p > 0.05$). Furthermore, Fig. 6b illustrates the surface wettability of both the bare and PG–PEI-coated wood blocks. The unpaired *t*-test results revealed a significant difference ($p < 0.001$) between the PG–PEI-coated sample and the bare wood. This suggests that the PG–PEI coating alters the surface wettability of wood blocks, making them slightly more hydrophilic. These findings indicate that the PG–PEI coating minimally affects the water uptake behavior of the wood, thus preserving its natural moisture-related functions.

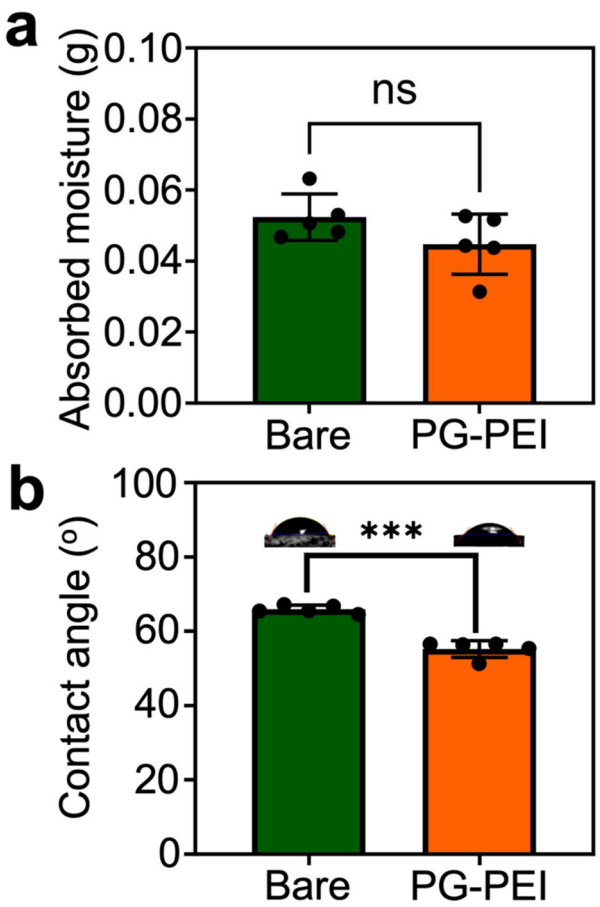

Fig. 6 (a) Unpaired *t*-test results for the hydration levels of the bare and PG–PEI-coated woods. (b) Unpaired *t*-test results for the water contact angles of the bare and PG–PEI-coated wood blocks. (***: $p < 0.001$, $n = 5$).

The stability of the PG–PEI coating is crucial for ensuring long-term effectiveness and allowing trees to remain protected without requiring frequent reapplication. Therefore, the integrity of the PG–PEI coating was evaluated by monitoring changes in its color intensity over time. Fig. 7a shows the application of the PG–PEI coating on a pine tree (*Pinus koraiensis*). A minimal lightening of the color intensity was observed after 70 days of exposure to environmental conditions, indicating that the coating remained largely intact after the exposure. To quantitatively assess the level of coating degradation, a smartphone app called Color Picker was used to measure the RGB values of the coatings, as shown in Fig. 7b. The formula $(IB_{Blank} - IB)/255$ was used to calculate the color intensity of the coatings (an unpaired *t*-test was conducted to compare the color intensity between day 1 and day 70). The color intensity on day 1 served as the baseline for statistical analysis, with measurements taken at 14 day intervals. The unpaired *t*-test results revealed a minimal difference ($p > 0.05$) in color inten-

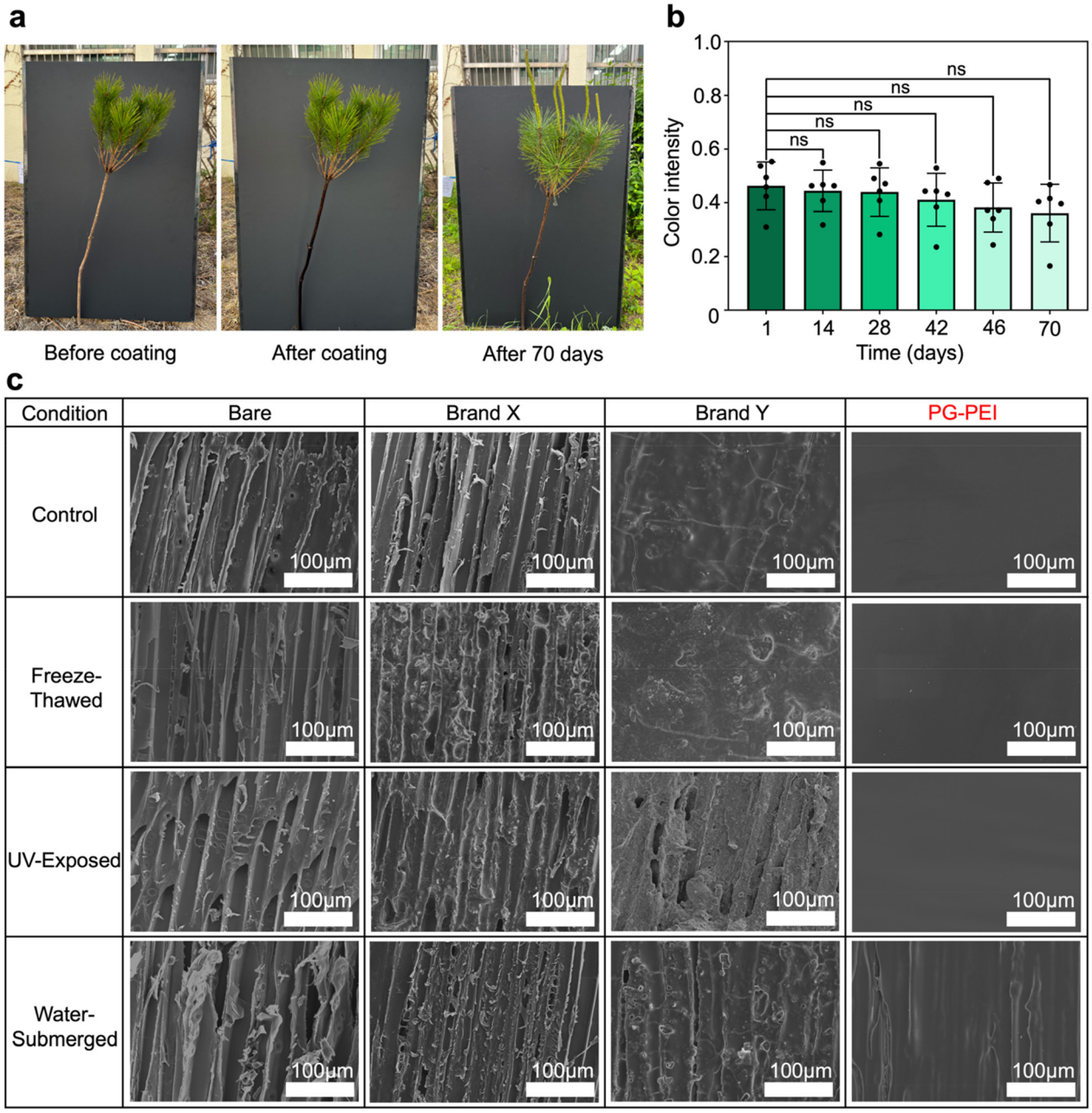

Fig. 7 (a) Photographs of a Korean pine tree (*Pinus koraiensis*) in its initial state, after being coated with PG–PEI, and after 70 days of coating. (b) Unpaired *t*-test results of the color intensity of the coating from day 1 to day 70; the day 1 data was used as the reference for statistical analysis (ns: $p > 0.05$, $n = 6$). (c) SEM images of bare wood, Brand X-coated wood, Brand Y-coated wood, and PG–PEI-coated wood blocks after exposure to various simulated weathering conditions (freeze-thaw cycles, UV exposure, and water submersion). Unexposed control samples were also shown for comparison.

sity between the day 1 sample and those collected up to day 70. This indicates that although there was a visible reduction in color intensity, the degradation was not statistically significant to suggest a substantial loss of the coating.

The observed lightening of the color intensity can be attributed to various environmental factors, including rainfall, UV radiation, wind exposure, and other weathering elements. Despite these environmental challenges, the statistical analysis indicated that the PG–PEI coating remained relatively stable over the 70 day period. The lack of a significant difference in color intensity over time suggests that the coating continued to adhere effectively to the tree surface even though it visually appeared lighter. This persistence is critical, as it demonstrates that the PG–PEI coating maintains its protective benefits for an extended period, even under adverse environmental conditions.

To further evaluate the durability of the PG–PEI coating under environmental stresses, differently coated wood blocks were exposed to simulated weathering conditions, including freeze-thaw cycles, UV exposure, and water submersion. High-magnification SEM images reveal the structural changes induced by these harsh environments (Fig. 7c). Despite having no protective layer, bare wood showed negligible structural alterations, underscoring its inherent resistance to environmental stressors. SEM images of Brand X-coated wood revealed an incomplete, non-uniform coating that failed to form an effective protective layer, causing changes similar to those of bare wood under all weathering conditions. Meanwhile, Brand Y-coated wood demonstrated a more uniform surface with minor cracking, indicating a successful initial coating. However, it underwent substantial degradation in every weathering scenario: freeze-thaw cycles and UV exposure caused surface roughening, and water submersion led to swelling, coating breakdown, and eventual detachment. The PG–PEI-coated samples displayed exceptional stability across all conditions. Although slight swelling occurred under water submersion, the coating remained intact without any signs of breakdown or delamination. Overall, these findings suggest that PG–PEI forms a durable, robust protective layer capable of effectively mitigating environmental degradation, surpassing the performance of other conventional coatings and offering superior long-term durability for wood-based materials under harsh conditions.

Finally, the survival of the pine trees (*Pinus koraiensis*) was monitored over 12 weeks to evaluate how it was affected by the PG–PEI coating. As shown in Fig. 8a, both the bare and PG–PEI-coated trees exhibited a 100% survival rate over 12 weeks, indicating that the coating had no adverse effects on the trees. This result suggests that the PG–PEI coating does not negatively affect the physiological processes required for tree survival, confirming its suitability for protective applications.

To further assess the biocompatibility of the PG–PEI coating with neighboring living organisms, a cytotoxicity test was conducted using the CCK-8 assay (Fig. 8b). The assay was performed with different coating concentrations of 1.25 mg mL^{-1}, 0.625 mg mL^{-1}, and 0.313 mg mL^{-1}, which represent high concentrations for *in vitro* studies. The results demonstrated that the PG–PEI coating exhibited high biocompatibil-

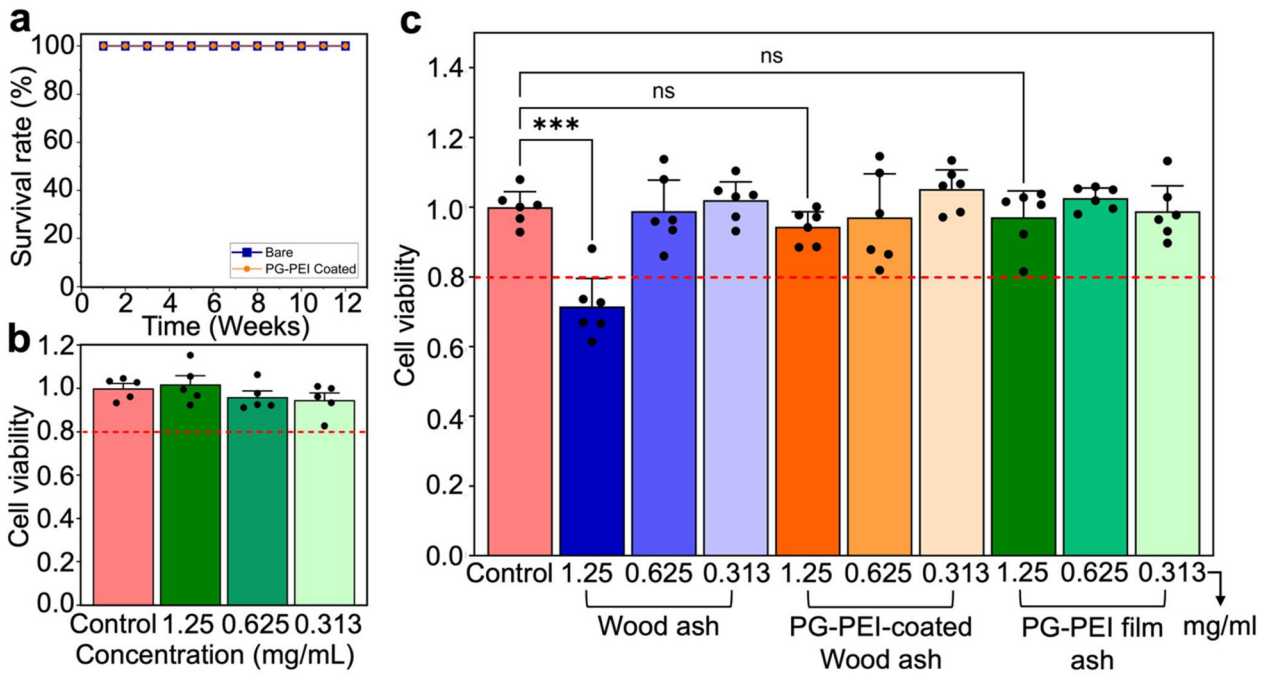

Fig. 8 (a) Survival rates of the bare and PG–PEI-coated Korean pine trees (*Pinus koraiensis*) over 12 weeks (control: $n = 5$; coated: $n = 6$). (b) Cell viability test results of the PG–PEI film at concentrations of 1.25, 0.625, and 0.313 mg mL^{-1} (cytotoxicity threshold: <80%). (c) Cell viability of wood ash, PG–PEI-coated wood ash, and PG–PEI film ash at 1.25, 0.625, and 0.313 mg mL^{-1} (cytotoxicity threshold: <80%; ns: $p > 0.05$, ***: $p < 0.001$, $n = 6$).

ity, with the cell viability remaining well above 80% across all tested concentrations. Therefore, this coating can be considered nontoxic to living cells, indicating its biocompatibility and suitability for safe application to trees and the surrounding ecosystem.

It is also crucial to evaluate whether PG–PEI releases biologically harmful substances upon burning. In this context, Fig. 8C presents the CCK-8 assay results for wood ash, PG–PEI-coated wood ash, and PG–PEI film ash at concentrations of 1.25, 0.625, and 0.313 mg mL^{-1}. Compared to the control (no treatment), all samples exhibited biocompatible behavior at or below 0.625 mg mL^{-1}. At the higher concentration (1.25 mg mL^{-1}), wood ash showed significant toxicity ($p < 0.001$), whereas both PG–PEI-coated wood ash and PG–PEI film ash remained non-toxic at all tested concentrations (non-significant p-values). This result indicates that PG–PEI-derived ash has lower toxicity than bare wood ash, underscoring PG–PEI's ability to mitigate toxicity even upon combustion. Consequently, PG–PEI not only avoids releasing harmful substances but also produces less toxic ash, highlighting its potential as a safe, sustainable coating for trees.

For additional evidence of PG–PEI's environmental friendliness, we performed ICP-OES analysis on extracts from bare, Brand X-, Brand Y-, and PG–PEI-coated wood after water exposure (Table S1†). Brand X contained iron, manganese, aluminum, and a high level of phosphorus (452 ppm), whereas Brand Y showed only trace manganese and moderate phosphorus (2.03 ppm). In contrast, PG–PEI was essentially metal- and phosphorus-free, with negligible traces likely due to contamination. Because metal- or phosphorus-based fire retardants can persist in soil and water, exceed toxicity thresholds, harm wildlife, and disrupt ecosystems,[45–47] these findings underscore PG–PEI's reduced environmental impact and its potential as a safer, more sustainable alternative. In this context, GC chromatograms further highlight the coating's environmental friendliness (Fig. S7†). Burned bare wood exhibited GC peaks primarily associated with cellulose and lignin derivatives, while burned PG–PEI-coated samples showed a similar profile, indicating no substantial difference in gaseous composition. Notably, no toxic VOCs were detected within the 0–20 minute retention time range, indicating that PG–PEI provides fire-retardant protection without posing additional risks to air quality.

Conclusions

We have developed a novel coating that effectively retards fire, offering an environmentally friendly, cost-effective, non-invasive, durable, and biocompatible solution. This innovative coating, which comprises a 1 : 1 ratio of PG and PEI, can be spray-coated on trees in an oxygen-rich environment. Upon exposure to high temperatures, the coating undergoes graphitization, significantly enhancing the thermal stability of the trees. This process not only helps to retard fire but also contributes to the overall protection of natural ecosystems and human communities in fire-prone areas. Our research findings indicate that this PG–PEI coating method offers a sustainable and practical approach to wildfire prevention and mitigation. This coating has the potential to reduce the spread of wildfires by improving the thermal stability of trees, thereby safeguarding both the environment and residential areas. Furthermore, the biocompatibility and environmental friendliness of the coating ensures that it does not harm the trees or the surrounding ecosystem, making it a promising advancement in fire-retardant technologies.

Author contributions

Conceptualization, M. J. C., K. L.; methodology, M. J. C., J. K., K. L.; investigation, M. J. C., J. K., K. L.; data curation, M. J. C., J. K., K. L.; formal analysis, M. J. C., J. K., J. L., M. P., K. L.; validation, M. J. C., J. K., J. L., M. P., K. L.; visualization, M. J. C., K. L.; writing – original draft, M. J. C., K. L.; writing – review and editing, M. J. C., J. K., J. L., M. P., K. L.; funding acquisition, K. L.; project administration, K. L.; resources, K. L.; supervision, M. P., K. L. All authors have read and agreed to the submitted version of the manuscript.

Data availability

The data supporting the findings of this study are provided within the article, with additional details available in the ESI.†

Conflicts of interest

The authors declare the following financial interests/personal relationships which may be considered as potential competing interests: M. J. C. and K. L. have a patent pending to Kyungpook National University.

Acknowledgements

This research was supported by grants of the National Research Foundation of Korea (NRF) grant funded by the Korea government (MSIT) (No. RS-2023-00212797), and Global – Learning & Academic research institution for Master's·PhD students, and Postdocs (LAMP) Program of the National Research Foundation of Korea (NRF) grant funded by the Ministry of Education (No. RS-2023-00301914).

References

1 A. Duane, M. Castellnou and L. Brotons, *Clim. Change*, 2021, **165**, 43.
2 E. Ponomarev, N. Yakimov, T. Ponomareva, O. Yakubailik and S. G. Conard, *Atmosphere*, 2021, **12**, 1–43.

3 I. R. van der Velde, G. R. van der Werf, S. Houweling, J. D. Maasakkers, T. Borsdorff, J. Landgraf, P. Tol, T. A. van Kempen, R. van Hees, R. Hoogeveen, J. P. Veefkind and I. Aben, *Nature*, 2021, **597**, 366–369.
4 D. Nimmo, A. Carthey, C. Jolly and D. Blumstein, *Global Change Biol.*, 2021, **27**, 5684–5693.
5 J. Pickrell and E. Pennisi, *Science*, 2020, **370**, 18–19.
6 A. Àgueda, E. Pastor and E. Planas, *Prog. Energy Combust. Sci.*, 2008, **34**, 782–796.
7 H. Nabipour, H. Shi, X. Wang, X. Hu, L. Song and Y. Hu, *Fire Technol.*, 2022, **58**, 2077–2091.
8 W. Cho, J. R. Shields, L. Dubrulle, K. Wakeman, A. Bhattarai, M. Zammarano and D. M. Fox, *Polym. Degrad. Stab.*, 2022, **197**, 109870.
9 R. A. Ilyas, S. M. Sapuan, M. R. M. Asyraf, D. A. Z. N. Dayana, J. J. N. Amelia, M. S. A. Rani, M. N. Norrrahim, N. M. Nurazzi, H. A. Aisyah, S. Sharma, M. R. Ishak, M. Rafidah and M. R. Razman, *Polymers*, 2021, **13**, 1326.
10 S. Araby, B. Philips, Q. Meng, J. Ma, T. Laoui and C. H. Wang, *Composites, Part B*, 2021, **212**, 108675.
11 J. Gao, Y. Wu, J. Li, X. Peng, D. Yin, H. Jin, S. Wang, J. Wang, X. Wang, M. Jin and Z. Yao, *Composites, Part C*, 2022, **9**, 100297.
12 Y. Huang, T. Ma, L. Li, Q. Wang and C. Guo, *Prog. Org. Coat.*, 2022, **172**, 107104.
13 X. Jiao, Y. Song, N. He, S. Shi, L. Xie, X. Wang, D. Hu, M. Li, G. Lai and X. Yang, *Prog. Org. Coat.*, 2022, **173**, 107169.
14 C. Yan, Y. Fang, R. Yang, M. Yan, W. Wang, Y. Song and Q. Wang, *Prog. Org. Coat.*, 2025, **200**, 109037.
15 S. Yang, Z. Liu, Z. Wang, Y. Wu and N. Ji, *J. Build. Eng.*, 2023, **73**, 106676.
16 C. A. Moody, G. N. Hebert, S. H. Strauss and J. A. Field, *J. Environ. Monit.*, 2003, **5**, 341–345.
17 X. C. Hu, D. Q. Andrews, A. B. Lindstrom, T. A. Bruton, L. A. Schaider, P. Grandjean, R. Lohmann, C. C. Carignan, A. Blum, S. A. Balan, C. P. Higgins and E. M. Sunderland, *Environ. Sci. Technol. Lett.*, 2016, **3**, 344–350.
18 C. A. Moody and J. A. Field, *Environ. Sci. Technol.*, 2000, **34**, 3864–3870.
19 Y. V. Pas'ko and O. P. Machneva, *Polym. Sci., Ser. D*, 2019, **12**, 283–285.
20 C. M. Popescu and A. Pfriem, *Fire Mater.*, 2019, **44**, 100–111.
21 A. C. Yu, H. L. Hernandez, A. H. Kim, L. M. Stapleton, R. J. Brand, E. T. Mellor, C. P. Bauer, G. D. McCurdy, A. J. Wolff 3rd, D. Chan, C. S. Criddle, J. D. Acosta and E. A. Appel, *Proc. Natl. Acad. Sci. U. S. A.*, 2019, **116**, 20820–20827.
22 G. E. Hengst and J. O. Dawson, *Can. J. For. Res.*, 1994, **24**, 688–696.
23 M. Á. Cárdenas-Gutiérrez, F. E. Pedraza-Bucio, P. Lopez-Albarran, J. G. Rutiaga-Quiñones, F. Correa-Mendez, A. Carrillo-Parra and R. Herrera-Bucio, *Wood Res.*, 2018, **63**, 795–808.
24 H. Tribusch and S. Fiechter, *WIT Trans. Built Environ.*, 2008, **97**, 43–52.
25 F. Yao, C. Zhai, H. Wang and J. Tao, *IOP Conf. Ser.: Earth Environ. Sci.*, 2018, **121**, 022016.
26 K. Lee, E. Prajatelistia, D. S. Hwang and H. Lee, *Chem. Mater.*, 2015, **27**, 6478–6481.
27 Y. Wang, J. P. Park, S. H. Hong and H. Lee, *Adv. Mater.*, 2016, **28**, 9961–9968.
28 Y. Wang, E. J. Jeon, J. Lee, H. Hwang, S. W. Cho and H. Lee, *Adv. Mater.*, 2020, **32**, 2002118.
29 H. Choi and K. Lee, *Appl. Sci.*, 2022, **12**, 11626.
30 J. E. Chung, S. Tan, S. J. Gao, N. Yongvongsoontorn, S. H. Kim, J. H. Lee, H. S. Choi, H. Yano, L. Zhuo, M. Kurisawa and J. Y. Ying, *Nat. Nanotechnol.*, 2014, **9**, 907–912.
31 M. Shin, H. A. Lee, M. Lee, Y. Shin, J. J. Song, S. W. Kang, D. H. Nam, E. J. Jeon, M. Cho, M. Do, S. Park, M. S. Lee, J. H. Jang, S. W. Cho, K. S. Kim and H. Lee, *Nat. Biomed. Eng.*, 2018, **2**, 304–317.
32 H. Shagholani and S. M. Ghoreishi, *J. Drug Delivery Sci. Technol.*, 2017, **39**, 88–94.
33 Y. Lee, K. Jun, K. Lee, Y. C. Seo, C. Jeong, M. Kim, I. K. Oh and H. Lee, *Angew. Chem.*, 2020, **132**, 3892–3898.
34 S. Ryu, J. B. Chou, K. Lee, D. Lee, S. H. Hong, R. Zhao, H. Lee and S. G. Kim, *Adv. Mater.*, 2015, **27**, 3250–3255.
35 Y. Yan, S. Dong, H. Jiang, B. Hou, Z. Wang and C. Jin, *ACS Omega*, 2022, **7**, 29369–29379.
36 J. Wu, W. Wang and Z. Wang, *Nanomaterials*, 2020, **10**, 326.
37 A. Y. Lee, D. M. Blakeslee, C. J. Powell and J. J. R. Rumble, *Data Sci. J.*, 2002, **1**, 1–12.
38 J. Y. Lee, N. Y. Kim, D. Y. Shin, H.-Y. Park, S.-S. Lee, S. J. Kwon, D.-H. Lim, K. W. Bong, J. G. Son and J. Y. Kim, *J. Nanopart. Res.*, 2017, **19**, 98.
39 C. Duong-Viet, H. Ba, L. Truong-Phuoc, Y. Liu, J.-P. Tessonnier, J.-M. Nhut, P. Granger and C. Pham-Huu, in *New Materials for Catalytic Applications*, ed. V. I. Parvulescu and E. Kemnitz, Elsevier, Amsterdam, 2016, vol. 1, pp. 273–311.
40 N. Talukder, Y. Wang, B. B. Nunna and E. S. Lee, *Carbon*, 2021, **185**, 198–214.
41 P. G. Gan, S. T. Sam, M. F. b. Abdullah and M. F. Omar, *J. Appl. Polym. Sci.*, 2019, **137**, 48544.
42 K. Lee, M. Park, K. G. Malollari, J. Shin, S. M. Winkler, Y. Zheng, J. H. Park, C. P. Grigoropoulos and P. B. Messersmith, *Nat. Commun.*, 2020, **11**, 4848.
43 B.-H. Lee, H.-S. Kim, S. Kim, H.-J. Kim, B. Lee, Y. Deng, Q. Feng and J. Luo, *Constr. Build. Mater.*, 2011, **25**, 3044–3050.
44 Q. Liu, Y. Chai, N. Lin and W. Lyu, *Materials*, 2020, **13**, 4478.
45 M. H. Schammel, S. J. Gold and D. L. McCurry, *Environ. Sci. Technol. Lett.*, 2024, **11**, 1247–1253.
46 A. Yu, M. Reinhart, R. Hunter, K. Lu, C. Maikawa, N. Rajakaruna, J. Acosta, C. Stubler, C. Appel and E. Appel, *Environ. Sci. Technol.*, 2021, **55**, 2316–2323.
47 K. D. Rock, G. St Armour, B. Horman, A. Phillips, M. Ruis, A. K. Stewart, D. Jima, D. C. Muddiman, H. M. Stapleton and H. B. Patisaul, *Toxicol. Sci.*, 2020, **176**, 203–223.